Anal. Chem. **2005,** *77,* 5107−5113

Label-Free Electrochemical Detection for Aptamer-Based Array Electrodes

Danke Xu,* Dawei Xu,† Xiaobo Yu,† Zhihong Liu, Wei He, and Zhenqiu Ma‡

Department of Biochemistry, Beijing Institute of Radiation Medicine, Beijing 100850, China

An electrochemical impedance spectroscopy method of detection for aptamer-based array electrodes is reported in which the binding of aptamers immobilized on gold electrodes leads to impedance changes associated with target protein binding events. Human IgE was used as a model target protein and incubated with the aptamer-based array consisting of single-stranded DNA containing a hairpin loop. To increase the binding efficiency for proteins, a hybrid modified layer containing aptamers and cysteamine was fabricated on the photolithographic gold surface through molecular self-assembly. Atomic force microscopy analysis demonstrated that human IgE could be specifically captured by the aptamer and stand well above the self-assembled monolayer (SAM) surface. Compared to immunosensing methods using anti-human IgE antibody as the recognition element, impedance spectroscopy detection could provide higher sensitivity and better selectivity for aptamer-modified electrodes. The results of this method show good correlation for human IgE in the range of 2.5−100 nM. A detection limit of 0.1 nM (5 fmol in a 50-μL sample) was obtained, and an average of the relative standard deviation was <10%. The method herein describes the first label-free detection for arrayed electrodes utilizing electrochemical impedance spectroscopy.

Over the past decade, nucleic acid biosensing methods based on the sequence-selective principle have enabled rapid advances in the development of many fields, from the rapid identification of DNA or the analysis of single nucleotide polymorphisms to the diagnosis of many genetic diseases.[1−3] Compared to enzymes or antibodies, nucleic acids have more advantages, such as their facile synthesis and modification, higher stability, and lower cost. Accordingly, DNA sensors have recently been developed into DNA microarrays[4,5] as well as into DNA biochips.[6,7] However, the utilization of this powerful tool is largely limited to genetic analysis. More recently, aptamer sensors as new molecular recognition devices in which nucleic acids provide another approach for selective binding to target proteins or enzymes based on their defined tertiary structures have gained considerable attention.[8−12] Although aptamers are the DNA or RNA ligands, they have demonstrated stronger and more selective affinity for protein targets compared to antibodies. As a result, aptamers are expected to become a powerful tool for proteome analysis due to the large number of affinity reagents necessary for proteome research.[13,14] Meanwhile, it is particularly important to develop label-free detection methods to avoid disturbances from conjugated markers and reduce operator procedure. They will be applied to the rapid screening of the interaction between DNA and proteins and the discovery of more novel aptamers, as well as to the design and fabrication of aptamer sensors.

In recent years, the detection methods of label-free, aptamer-based biosensors wherein the aptamers were immobilized on the solid supported material and the interaction between proteins and aptamers could be assayed have received an increasing amount of attention. Potyrailo et al. employed immobilized aptamers to specifically detect nonlabeled thrombin using the evanescent-wave-induced fluorescence anisotropy.[15] However, the aptamers have to be modified with a fluorescein label and amino-modified linkers such that the signal of a concomitant change would be obtained after forming the complex of the aptamer and the protein. Liss et al. described a quartz crystal microbalance (QCM) biosensor based on aptamers[12] in which they functionalized the gold surface

* Corresponding author. Phone/fax: +86-10-66932225. E-mail: xudk@nic.bmi.ac.cn.

† Present address: College of Veterinary Medicine, Northeast Agricultural University, Harbin, 150030 China.

‡ Present address: Department of Basic Medical Sciences, Zhejiang University, Hangzhou, 310031 China.

(1) Piunno, P. A. E.; Krull, U. J.; Hudson, R. H. E.; Damha, M. J.; Cohen, H. *Anal. Chem.* **1995**, *67*, 2635−2643.
(2) Wang, J.; Xu, D.; Kawde, A.-N.; Polsky, R. *Anal. Chem.* **2001**, *73*, 5576−5581.
(3) Drummond, T. G.; Hill, M. G.; Barton, J. K. *Nat. Biotechnol.* **2003**, *21* (10), 1192−1199.
(4) Bao, P.; Frutos, A. G.; Greef, C.; Lahiri, J.; Muller, U.; Peterson, T. C.; Warden, L.; Xie, X. *Anal. Chem.* **2002**, *74*, 1792−1797.
(5) Stenger, D. A.; Andreadis, J. D.; Vora, G. J.; Pancrazio, J. J. *Curr. Opin. Biotechnol.* **2002**, *13*, 208−212.
(6) Trau, D.; Lee, T. M. H.; Lao, A. I. K.; Lenigk, R.; Hsing, I.-M.; Ip, N. Y.; Carles, M. C.; Sucher, N. J. *Anal. Chem.* **2002**, *74*, 3168−3173.
(7) Weidenhammer, E. M.; Kahl, B. F.; Wang, L.; Wang, L.; Duhon, M.; Jackson, J. A.; Slater, M.; Xu, X. *Clin. Chem.* **2002**, *48* (11), 1873−1882.
(8) Savran, C.; Knudsen, S. M.; Ellington, A. D.; Manalis, S. R. *Anal. Chem.* **2004**, *76*, 3194−3198.
(9) Ho, H. A.; Leclerc, M. *J. Am. Chem. Soc.* **2004**, *126*, 1384−1387.
(10) Pavlov, V.; Xiao, Y.; Shlyahovsky, B.; Willner, I. *J. Am. Chem. Soc.* **2004**, *126*, 11768−11769.
(11) McCauley, T. G.; Hamaguchi, N.; Stanton, M. *Anal. Biochem.* **2003**, *319*, 244−250.
(12) Liss, M.; Petersen, B.; Wolf, H.; Prohaska, E. *Anal. Chem.* **2002**, *74*, 4488−4495.
(13) Famulok, M.; Mayer, G.; Blind, M. *Acc. Chem. Res.* **2000**, *33*, 591−599.
(14) Cox, J. C.; Hayhurst, A.; Hesselberth, J.; Bayer, T. S.; Georgiou, G.; Ellington, A. D. *Nucleic Acids Res.* **2002**, *30*, e108.
(15) Potyrailo, R. A.; Conrad, R. C.; Ellington, A. D.; Hieftje, G. M. *Anal. Chem.* **1998**, *70*, 3419−3425.

10.1021/ac050192m CCC: $30.25
Published on Web 07/08/2005

using streptavidin and the resulting layer was coupled with the biotin-labeled aptamer. The biosensor was shown to specifically detect protein by its natural frequency shifts. More recently, the direct analytical methods based on aptamers were further developed to atomic force microscopy[16] and surface stress-induced bending detection.[8] The former was used to investigate specific aptamer−protein interactions, and the latter method presented a microfabricated cantilever-based sensor.

Herein, we have developed a novel biosensing approach for aptamers that is based on electrochemical impedance spectroscopy (EIS). Electrochemical detection schemes are considered cost-effective alternatives to well-established optical read-outs because they offer high sensitivity using simple instrumentation that is compatible with microfabrication technology.[17−19] EIS is also one of the label-free electroanalytical approaches, wherein high sensitivity and the simple assay procedure of EIS make it extremely attractive for electrochemical biosensing methods.[20−24] However, to date, this detection approach has not been developed to assay aptamer-based electrodes.

In this paper, we selected human IgE and the relative aptamer as a receptor−ligand model system, in which the aptamer, functioning as the recognition element, was immobilized on the photolithographic gold film electrode via self-assembly. Initially, the specificity and sensitivity of EIS detection for the interaction between proteins and aptamers was investigated. Compared with typical impedimetric affinity sensors, in which immobilized antibodies are used as the recognition element on the electrodes, the aptamer-based electrodes have more advantages, such as lower background noise, decreased nonspecific adsorption, and larger differences in the impedance signals due to the small size and simple structure of the aptamers. In this contribution, these phenomena were further confirmed by atomic force microscopy (AFM) measurements. Additionally, we demonstrated that the hybrid modification by the addition of relatively small compounds containing a mercapto group gave rise to characteristic changes in affinity binding efficiency. Furthermore, an aptamer-based array electrode was explored to be assayed using EIS, and the specificity of recognizing the protein target was shown to be strongly dependent on the sequences of the aptamers. To our knowledge, this is the first example of using electrochemical impedance spectroscopy for aptamer-modified electrodes. The present detection method demonstrates its potential application for the direct detection of the interaction between aptamers and proteins as well as the fabrication of novel aptamer-based array biosensors.

(16) Jiang, Y.; Fang, X. H.; Bai, C. L. *Anal. Chem.* **2004**, *76*, 5230−5235.
(17) Ruan, C.; Yang, L. J.; Li, Y. *Anal. Chem.* **2002**, *74*, 4814−4820.
(18) Zayats, M.; Raitman, O. A.; Chegel, V. I.; Kharitonov, A. B.; Willner, I. *Anal. Chem.* **2002**, *74*, 4763−4773.
(19) Yang, L.; Li, Y.; Griffis, C. L.; Johnson, M. G. *Biosens. Bioelectron.* **2004**, *19*, 1139−1147.
(20) Dijksma, M.; Kamp, B.; Hoogvliet, J. C.; van Bennekom, W. P. *Anal. Chem.* **2001**, *73*, 901−907.
(21) Sadik, O. A.; Xu, H.; Gheorghiu, E.; Andreescu, D.; Balut, C.; Gheorghiu, M.; Bratu, D. *Anal. Chem.* **2002**, *74*, 3142−3150.
(22) Darain, F.; Park, D. S.; Park, J. S.; Shim, Y. B. *Biosens. Bioelectron.* **2004**, *19*, 1245−1252.
(23) Wang, M. J.; Wang, L. Y.; Wang, G.; Ji, X. B.; Bai, Y. B.; Li, T. J.; Gong, S. Y.; Li, J. H. *Biosens. Bioelectron.* **2004**, *19*, 575−582.
(24) Cai, W.; Peck, J. R.; van der Weide, D. W.; Hamers, R. J. *Biosens. Bioelectron.* **2004**, *19*, 1013−019.

EXPERIMENTAL SECTION

Materials. Immunoglobulin E purified from human plasma was purchased from US Biological Inc. (Swampscott, MA). Anti-human IgE antibody (ϵ-chain-specific) developed in goat fractionated antiserum and bovine serum albumin (BSA) were purchased from Sigma (St. Louis, MO). Cysteamine, *N*-acetyl-L-cysteine, 1-ethyl-3-(-3-dimethylaminopropyl) carbodiimide (EDC) and *N*-hydroxysuccinimide (NHS) were also purchased from Sigma. 1,4-Dithiothreitol (DTT) was obtained from Sino-America Bioengineering Co. (Beijing, China). Other chemicals were of analytical reagent grade. All samples and buffers were prepared using deionized water obtained from a Milli-Q water purification system.

The DNA aptamer, its complementary oligomer, and the scrambled sequences were all custom-synthesized from Sagon Co. (Shanghai, China), and their base sequences are as follows:

Sequence I (thiol-modified DNA aptamer): 5′-SH-GGG GCA CGT TTA TCC GTC CCT CCT A GT GGC GTG CCC C-3′

Oligomer complementary to the aptamer: 5′-GGG GCA CGC CAC TAG GAG GGA CGG ATA AAC GTG CCC C-3′

Sequence II: 5′-SH-GGG GCA CGT TTA TGG CTG GGT GGT A GT GGC GTG CCC C-3′

Sequence III: 5′-SH-GGG GCA CGT TTA TCC GAC CCA CCA TGT GGC GTG CCC C-3′

Sequence IV: 5′-SH-GGG GCA CGT TTA TCC GTT CCC TTC CTT A GT GGC GTG CCC C-3′

Instrumentation. All electrochemical impedance spectroscopy measurements were performed on a CHI 660 Electrochemical Workstation. (CH Instrumental Inc., Austin, USA). A two-electrode system consisted of the gold working electrode and a standard Ag/AgCl electrode, which served both as the counter and reference electrodes. All AFM experiments were performed using a SFM9500J3 (Shimadzu, Japan).

Array Electrode Chip Preparation. Construction of the arrayed electrode chip is shown in Figure 1. The electrode pattern was formed on a crystal wafer substrate (36 mm × 26 mm). A 200-nm-thick photolithographic gold film was prepared by vapor deposition, with an underlayer of chromium (50 Å) on the substrate. The dimension of each gold working electrode was 2 mm × 2 mm (Figure 1a). Prior to the modification, the chip was immersed in a piranha solution (H_2SO_4/H_2O_2, 3/1) for 30 min and then rinsed thoroughly using water and ethanol.

A home-constructed poly(dimethylsiloxane) (PDMS; Dow Corning Inc.) frame containing 24 microwells was then aligned onto the electrodes such that each well could exactly match the working electrodes, as shown in Figure 1b. Prior to the immobilization, a 10 μM solution of the aptamer or the scrambled sequences was mixed with 100 μM cysteamine (Tris−HCl buffer, pH 7.4; 1 mM EDTA, 0.2 M NaCl, and 100 mM DTT.). To modify the electrodes, the resulting solution was transferred into the relative microwells of the PDMS frame and subsequently incubated with the gold electrodes overnight. After the immobilization, the PDMS frame was removed, and the aptamer-modified chip was rinsed twice for 2 min each time in phosphate-buffered saline (PBS; 137 mM NaCl, 3 mM KCl, 10 mM phosphate, pH 7.4), followed by rinsing with deionized water. The rinsed chips were then dried under a stream of nitrogen. The port seals were attached onto the chip such that the whole chip would be divided into six incubation chambers, each chamber containing four

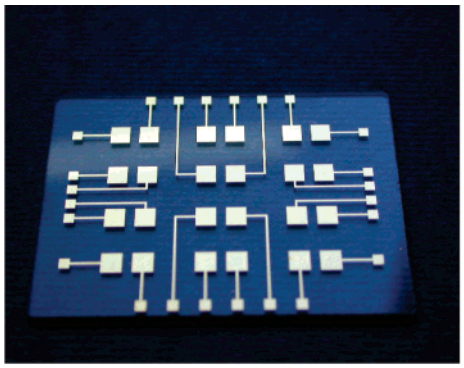

(a)

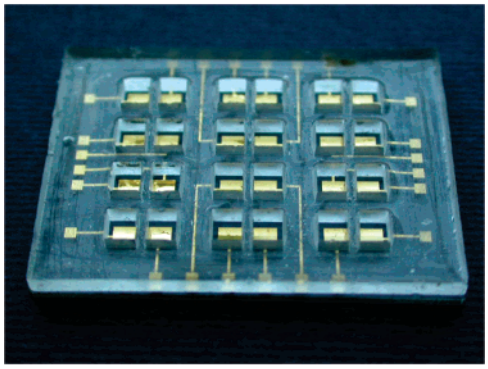

(b)

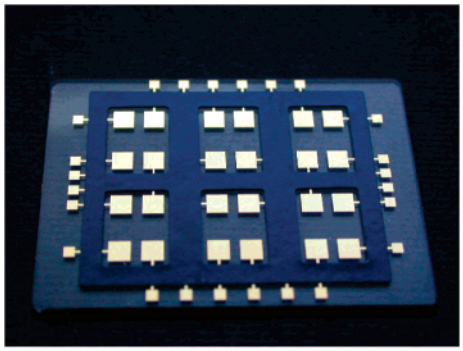

(c)

Figure 1. Construction of the gold array electrode chip: (a) a photolithographic gold film array electrode; (b) a home-constructed PDMS frame containing 24-microwells for the immobilization; (c) the array with six individual incubation chambers.

modified working electrodes (Figure 1c). In this case, one chip could be incubated with six samples, and each sample would be reacted with four modified electrodes simultaneously. In the experiment of arrayed electrode detection, the four electrodes in one chamber were modified with sequences I–IV, respectively. In other experiments, all electrodes on the chip were modified with the aptamer.

Procedure for the Detection of Proteins. To perform the experiments reported in this paper, 50 μL of protein samples were added into the incubation chamber using an Eppendorf pipet. The array electrodes were incubated with the samples for 1 h at room temperature, followed by rinsing with PBS buffer.

Impedance measurements were carried out on a CHI 660 Electrochemical Workstation using a two-electrode system. EIS data were simulated using the software CHI 660. Prior to the measurement, a 50-μL mixture containing 5.0 mM $[Fe(CN)_6]^{3-/4-}$ in 0.1 M KCl and 20 mM PBS was added into the detection chamber, followed by positioning an Ag/AgCl electrode into the chamber for detection. The frequency range investigated was from 1 to 100 kHz at the formal potential of 250 mV using an alternate voltage of 5 mV.

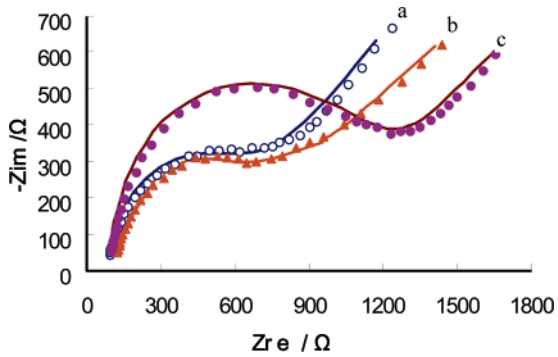

Figure 2. Nyquist diagram (Z_{im} vs Z_{re}) for the Faradaic impedance measurement in PBS buffer containing 5.0 mM $Fe(CN)_6^{3-/4-}$ (1:1 mixture) as the redox probe. (a) An aptamer-modified electrode, (b) the modified electrode after incubation with 50 nM human IgG, and (c) the modified electrode after incubation with 50 nM human IgE. The incubation time was 1 h. The impedance spectra were recorded within the range of 1–100 kHz at the formal potential of the $Fe(CN)_6^{3-/4-}$ redox couple. The amplitude of the alternate voltage was 5 mV. The symbols represent the experimental data, and the solid lines are the fitted curves using the equivalent circuit.

Immobilization of Anti-Human IgE Antibody. To make a comparison to antibody-based electrodes, an experiment was performed in which all gold electrodes on the chip were self-assembled with 10 mg/mL *N*-acetyl-L-cysteine for 4 h, followed by two water rinses. The resulting SAM-modified electrodes were further reacted with a mixture of 100 mg/mL EDC and 100 mg/mL NHS for 1 h. The reactive surface was incubated with 1 mg/mL anti-human IgE overnight. To deactivate and block the excess reactive groups remaining on the surface, 100 mM ethanolamine and 10 mg/mL BSA were added onto the resulting electrodes sequentially. The procedures of reaction with human IgE and the EIS measurement are the same as the previous section.

Atomic Force Microscopy Analysis. All AFM experiments were performed on a SFM9500J3 (Shimadzu, Japan). The AFM was carried out using the tapping mode. All images are presented without any subsequent data processing. Before performing the analysis, the electrodes were rinsed thoroughly with PBS and water to remove nonspecifically adsorbed antibodies and then dried with nitrogen. All AFM measurements were carried out in ambient air.

RESULTS AND DISCUSSION

Characterization of the Aptamer-Modified Gold Surface. The aptamer sequence specifically binding to human IgE used herein has been previously reported.[12,16,25] To covalently attach the aptamer to the gold surface and form an orientated self-assemblied monolayer, the 5′ end of the sequence was modified via a mercapto group. Figure 2 shows the results of impedance spectroscopy on the modified electrodes. It can be seen that the

(25) Wiegand, T. W.; Williams, P. B.; Dreskin, S. C.; Jouvin, M. H.; Kinet, J. P.; Tasset, D. *J. Immunol.* **1996**, *157*, 221–230.

Scheme 1. Equivalent Circuit Model for Complex Impedance Plots[a]

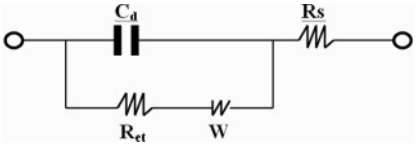

[a] R_s, solution resistance; C_d, double-layer capacitance; R_{et}, electron transfer resistance; W, Warburg impedance.

electrodes exhibit almost the same impedance spectra before and after the incubation with 50 nM human IgG (the control). When compared with the control, a significantly enlarged impedance curve was observed after the incubation with a 50 nM IgE sample. The impedance spectra follow the equivalent circuit described by Patolsky et al.,[26] as shown in Scheme 1. The circuit includes the ohmic resistance (R_s) of the electrolyte solution, Warburg impedance (W) resulting from the diffusion of ions from the bulk of the electrolyte to the interface, double-layer capacitance (C_d), and electron-transfer resistance (R_{et}). In fact, R_s and W are not affected by chemical transformations occurring at the electrode interface, since they represent bulk properties of the electrolyte solution and diffusion of the applied redox probe. Therefore, we use this equivalent circuit to fit the impedance spectra and to determine C_d and R_{et}. The capacitance (C_d) changes are not sensitive to the electron-transfer resistance. As a result, it can be expected that electron-transfer resistance is the most directive and sensitive parameter that responds to changes on the electrode interface. Whereas a linear section characteristic of the lower frequency is attributable to a diffusion-limited electron transfer, a squeezed semicircle portion observed at higher frequencies would correspond to the electron-transfer-limited process. It can be obtained from Figure 2 that the values of R_{et} of the impedance spectrum before and after the reaction with IgG were 452 Ω and 532 Ω, respectively. After the incubation with IgE, the R_{et} significantly increases to 978 Ω. This implies that IgE has been bound to the surface of the modified electrode.

Further confirmation of the interaction between the aptamer and human IgE was obtained from atomic force microscopy (AFM) measurements by a comparison of before and after the incubation of the aptamer-modified electrodes with human IgE (Figure 3). To observe the specificity of the aptamer for the protein, human IgG was employed as a control to incubate with the aptamer surface. To make a comparison between panels a, b, and c of Figure 3, the distinctive difference in the topography of the surface can be observed. When compared to the aptamer-modified electrode (Figure 3a), the AFM topographic image of the surface binding to human IgE shows clearly separated protein molecules, which stand well above the height of the aptamer-modified surface (Figure 3c). Although it can also be seen from Figure 3b that the AFM image shows some changes in the surface morphology after incubation of the aptamer surface with the IgG sample, there are no regular molecules appearing above the surface. In this case, the resulting increasing protein layer is probably caused by nonspecific adsorption. This is in agreement with the results from the impedance experiments.

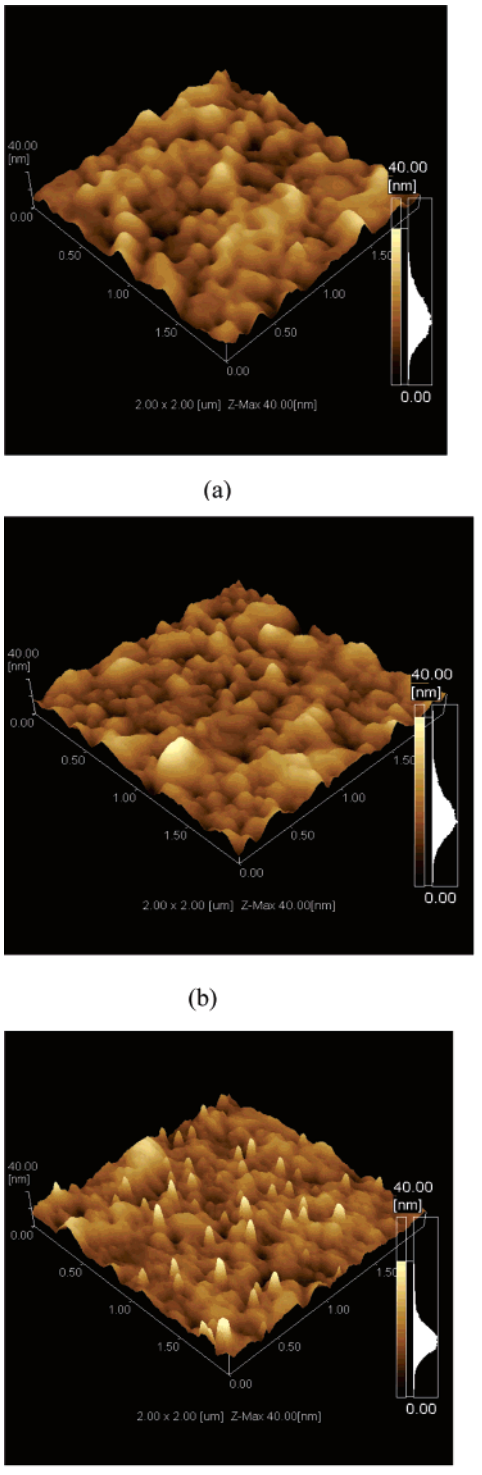

Figure 3. AFM images (2 μm × 2 μm) of (a) the aptamer-modified gold surface, (b) the modified electrode after incubation with 50 nM human IgG, and (c) the modified electrode after incubation with 50 nM human IgE.

To further compare its sensing properties with immunological sensors, the gold electrode was modified with the anti-human IgE antibody. Figure 4 shows impedance spectroscopy of the antibody-modified electrodes before and after binding 50 nM IgE. As can be seen, the diameter of the squeezed semicircle increases after incubation with the IgE sample. The results suggest that electron-transfer resistance on the electrode interface became higher due

(26) Patolsky, F.; Zayats, M.; Katz, B.; Willner, I. *Anal. Chem.* **1999**, *71*, 3171−3180.

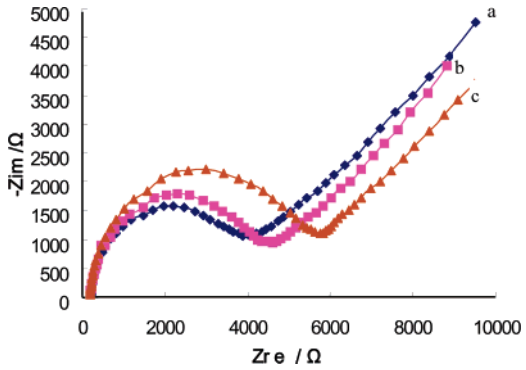

Figure 4. Nyquist diagram (Z_{im} vs Z_{re}) for the Faradaic impedance measurement in PBS buffer containing 5.0 mM $Fe(CN)_6^{3-/4-}$ (1:1 mixture) as the redox probe. (a) An anti-human IgE antibody-modified electrode, (b) the modified electrode after incubation with 50 nM human IgG, and (c) the modified electrode after incubation with 50 nM human IgE. The relative incubation time was 1 h. The impedance spectra were recorded within the range of 1−100 kHz at the formal potential of the $Fe(CN)_6^{3-/4-}$ redox couple. The amplitude of the alternate voltage was 5 mV. The symbols represent the experimental data, and the solid lines are the fitted curves using the equivalent circuit.

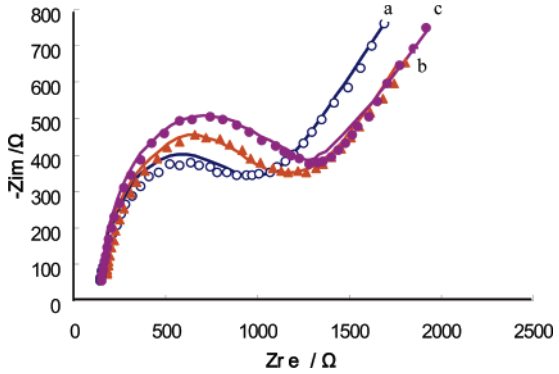

Figure 5. Nyquist diagram (Z_{im} vs Z_{re}) for the Faradaic impedance measurement in PBS buffer containing 5.0 mM $Fe(CN)_6^{3-/4-}$ (1:1 mixture) as the redox probe. (a) ds-DNA-modified electrode, (b) the modified electrode after incubation with 50 nM human IgG, and (c) the modified electrode after incubation with 50 nM human IgE. The relative incubation time was 1 h. The impedance spectra were recorded within the range of 1−100 kHz at the formal potential of the $Fe(CN)_6^{3-/4-}$ redox couple. The amplitude of the alternate voltage was 5 mV. The symbols represent the experimental data, and the solid lines are the fitted curves using the equivalent circuit.

to the formation of the antibody−antigen conjugated layer. However, the immunological sensor shows higher background relative to the aptamer sensor, which could lead to a decrease in its effective signals and its sensitivity.

In comparison, the aptamer has more advantages for EIS biosensors due to its smaller size and simple structure. First, aptamers can be easily modified with functional groups, such as mercapto or amino groups, at their ends in order to achieve a covalent orientation on the biosensing surface. Such a possibility has been demonstrated by our AFM analysis. The resulting surface not only increases the efficiency of binding proteins but also decreases the nonspecific adsorption, which is characteristic of most random immobilization of antibodies. Second, the small size of the aptamer means less electronic transfer resistance, producing a lower background for EIS measurement. In our experiments, when a 50 nM IgE sample was incubated with the

Table 1. The Influence of the Concentrations of Cysteamine in Aptamer Solution on the Capture Efficiency of the Modified Electrode[a]

	cysteamine concn (μM)				
	0	10	100	1000	5000
impedance Ω[a]	462 ± 12	860 ± 79	988 ± 110	827 ± 115	155 ± 19

[a] Impedance measurements were carried out in PBS buffer containing 5.0 mM $Fe(CN)_6^{3-/4-}$ (1:1 mixture) as the redox probe within the range of 1−100 kHz at the formal potential of the $Fe(CN)_6^{3-/4-}$ redox couple. The amplitude of the alternate voltage was 5 mV.

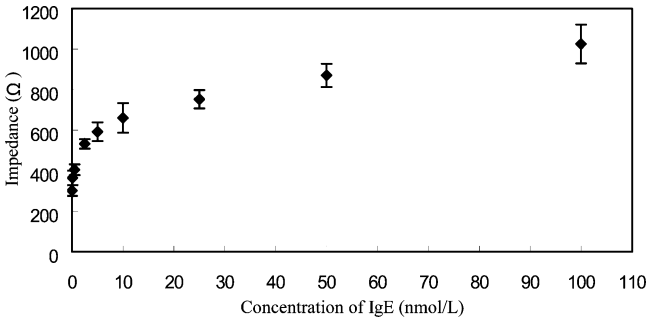

Figure 6. Dependence of impedance signal on concentrations of human IgE. The aptamer-modified electrodes were incubated with human IgE for 1 h. Impedance measurements were carried out in PBS buffer containing 5.0 mM $Fe(CN)_6^{3-/4-}$ (1:1 mixture) as the redox probe within the range of 1−100 kHz at the formal potential of the $Fe(CN)_6^{3-/4-}$ redox couple. The amplitude of the alternate voltage was 5 mV.

antibody-modified electrodes, the average impedance values were increased to 3602 Ω from 2530 Ω of the background. The detected signal increased by 42.4% relative to the background. The average impedance values of the aptamer-modified electrodes, on the other hand, were increased to 978 Ω from 452 Ω of the background, a 116.4% increasement relative to the background. Hence, impedance spectroscopy would be an extremely attractive detection approach for the aptamer-based biosensors.

Compared to nucleic acid sensors, the significant difference lies in that the principle of an aptamer's recognizing and binding to its target is dependent on its tertiary structures rather than merely its sequence of bases. A similar affinity phenomenon has been reported in the study of protein−DNA interactions.[27−29] In those cases, however, the recognizing and capture elements are typically ds-DNA of single-base mismatches. To provide further information concerning the recognizing elements, DNA duplexes containing the same sequence as the aptamer were used to modify the surface of the gold electrode. To hinder the aptamer from the tertiary structure of the hairpin loop, 10 μM aptamer solution was mixed in advance with a 10 μM solution of the complementary strand and then kept in a water bath at 100 °C for 10 min. This allowed the hairpin loop of the aptamer to be opened first, followed by the formation of the hybridized ds-DNA. The resulting solution was transferred to modify the electrodes. Figure 5 shows their

(27) Boon, E. M.; Salas, J. E.; Barton, J. K. *Nat. Biotechnol.* **2002**, *20*, 282−286.
(28) Long, Y. T.; Li, C. Z.; Sutherland, T. C.; Kraatz, H. B.; Lee, J. S. *Anal. Chem.* **2004**, *76*, 4059−4065.
(29) Li, C. Z.; Long, Y. T.; Lee, J. S.; Kraatz, H. B. *Chem. Commun.* **2004**, 574−575.

Scheme 2. The Estimated Secondary Structures of IgE DNA Aptamer(I); Sequence II in Which C and G in Its Hairpin Loop Were Exchanged for G and C, Respectively; Sequence III in Which A and T in Its Hairpin Loop Were Exchanged for T and A, Respectively; and Sequence IV in Which an Additional Three T Were Inserted into Its Hairpin Loop

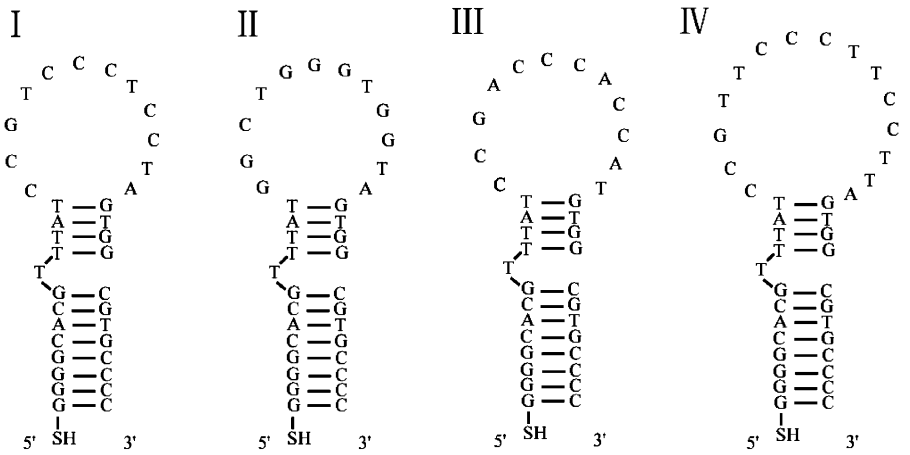

impedance spectra from the modified electrodes before and after incubation with the target human IgE. As expected, no significant difference could be obtained from such a biosensing surface. In addition, an increase in the diameter of the squeezed semicircle suggested that electron transfer resistance became somewhat higher than the aptamer-modified surface. This could be attributed to the formation of a tightly packed ds-DNA layer.

Optimization of Conditions. Surface modification is an important step for the fabrication of biosensors. It has been previously reported[30] that hybrid immobilization would be beneficial to increase binding efficiency owing to improvements in stereo hindrance. To further investigate its influence on the aptamer sensor, cysteamine was selected to be mixed with the aptamer solution prior to immobilization. The modified electrodes were further incubated with 50 nM human IgE for 1 h. The effect of the concentration of cysteamine on the binding efficiency is shown in Table 1. The results suggest that the ratio of 1:10 (the aptamer/cysteamine) was most appropriate for surface modification. The high ratio is necessary for formation of the aptamer−IgE complex.

Quantitative Analysis. We tested the quantitative ability of the aptamer-modified array electrodes based on EIS to assay human-IgE at various concentrations. The relationship of the impedance values and the concentrations of IgE is shown in Figure 6. The quantitative behavior was assessed by analyzing the dependence of the impedance signals upon the concentrations of the target protein human IgE. The target concentration was observed in the range of 2.5−100 nM, exhibiting a highly linear calibration curve with a correlation coefficient of 0.998. According to the optimization of the incubation conditions, a detection limit of ~0.1 nM (5 fmol in a 50-μL sample) was obtained on the basis of the signal-to-noise characteristics when the incubation time was increased to 90 min. A series of four repetitive measurements of IgE solution at concentrations of 0.1, 0.5, 2.5, 5.0, 10.0, 25.0, 50.0, and 100 nM was used for estimating the precision and yielded acceptable, reproducible signals. The average of the relative standard deviation was 7.66%.

(30) Abel, A. P.; Weller, M. G.; Duveneck, G. L.; Ehrat, M.; Widmer, H. M. *Anal. Chem.* **1996**, *68* (17), 2905−2912.

Table 2. Detection of the Arrayed Electrode[a]

	oligomers[a]			
	I	II	III	IV
impedance background (Ω) [b]	492 ± 46	410 ± 57	465 ± 60	460 ± 63
impedance signals (Ω) [c]	915 ± 49	445 ± 31	512 ± 72	504 ± 54

[a] The sequences of the oligomers I, II, III, and IV are shown in Scheme 2. [b] Impedance background determined by the gold electrodes modified with the relevant oligomer. [c] Impedance signals determined by the modified electrode after incubation with 50 nM human IgE.

Arrayed Electrode Detection. It has been reported[13,14] that aptamers could be used as capture reagents aimed at many relevant protein targets from biological samples. The development of aptamer-based arrays could accelerate the discovery of novel aptamers and their applications in clinical diagnosis as well as in proteomics research. Additionally, label-free detection is an ideal approach to confirm the interaction between aptamers and target proteins. To assess the EIS detection scheme for aptamer-based array electrodes, four oligomers with the characteristic forming hairpin loop were selected to fabricate the array. One of the oligomers (sequence I) is the aptamer to specifically bind human IgE, and the other sequences were somewhat changed, as shown in Scheme 2. The four oligomers were injected into the individual wells in the PDMS frame on the chip such that the reactive electrodes located in the same chamber were modified with the four oligomers. The background of the resulting array was first measured, and the results are shown in Table 2.

Almost the same impedance values from the four sequences imply that the EIS method could provide a constant baseline for the aptamers. In fact, it would be an essential condition for array detection because the label-free direct detection signals are highly dependent on the background. The array electrode was further incubated with 50 nM human IgE, and impedance signals in Table 2 show the detection profile. As expected, a significant increment in the impedance signal was obtained from the aptamer-modified electrode (the oligomer with sequence I). The results imply that

the affinity of the aptamer strongly depends not only on its loop size but also on its sequence. As demonstrated in this experiment, such a difference could be detected specifically and sensitively using the presented EIS method.

CONCLUSIONS

We have demonstrated an electrochemical impedance spectroscopy detection method for aptamer-modified array electrodes. Aptamers were successfully immobilized on the gold surface through a hybrid modification by addition of cysteamine, which exhibited rather significant improvements in stereo hindrance for binding to the target protein. The resulting surface binding with human IgE has been further characterized using AFM. When compared to the immunosensing system based on antibody modification, aptamer-based biosensors show more advantages in biosensing technology. First, aptamers could form an orientated modified layer through chemical modification. As a result, this not only significantly increases the efficiency of protein binding but also leads to a constant background due to the decrease of nonspecific adsorption. Second, the aptamer-based EIS sensor has a lower background due to its small molecular structure. Hybrid modification not only reduces electronic transfer resistance but also increases room for protein binding. Third, aptamer preparation and modification is quite facile, and the aptamers are more stable for storage. More importantly, these merits have been demonstrated to be appropriate for EIS biosensing, and we have further developed this method to be utilized in aptamer-based array electrodes. We have demonstrated that electrochemical impedance spectroscopy could be a promising label-free detection approach for aptamers in quantitative measurements as well as their screen analysis.

ACKNOWLEDGMENT

This work was supported by Hi-tech Research and Development Program of China (863 Program, No. 2002-BA711A11) and the National Basic Research Program of China (973 Program, No. 2004CB520804).

Received for review January 29, 2005. Accepted June 4, 2005.

AC050192M